Anomalous staged hot-electron acceleration by two-plasmon decay instability in magnetized plasmas

X. X. Li,[1] R. J. Cheng,[1] Qing Wang,[1] D. J. Liu[®],[1] S. Y. Lv,[1] Z. M. Huang,[1] S. T. Zhang,[1] X. M. Li,[1] Z. J. Chen,[2]
Qiang Wang,[1] Z. J. Liu,[1,3,*] L. H. Cao[®],[1,3] C. Y. Zheng,[1,3] and X. T. He[1,3]

[1]*Institute of Applied Physics and Computational Mathematics, Beijing 100094, China*
[2]*HEDPS, Center for Applied Physics and Technology, and State Key Laboratory of Nuclear Physics and Technology,
School of Physics, Peking University, Beijing 100871, China*
[3]*HEDPS, Center for Applied Physics and Technology, and College of Engineering, Peking University, Beijing 100871, China*

We present a staged hot-electron acceleration mechanism of the two-plasmon decay (TPD) instability in the transverse magnetic field under the parameters relevant to inertial confinement fusion experiments. After being accelerated by the forward electron plasma wave (FEPW) of TPD, the hot-electrons can be anomalously accelerated again by the backward electron plasma wave (BEPW) of TPD and then obtain higher energy. Moreover, the surfatron acceleration mechanism of TPD in the magnetic field is also confirmed, the electrons trapped by the TPD daughter EPWs are accelerated in the direction along the wave front. Interestingly, the velocity of electrons accelerated by surfing from the FEPW is quite easily close to the BEPW phase velocity, which markedly enhances the efficiency of the staged acceleration. The coexistence of these two acceleration mechanisms leads to a significant increase of energetic electrons generated by TPD in the magnetic field. Meanwhile the EPWs are dissipated, TPD instability is effectively suppressed, and the laser transmission increases.

In laser-driven inertial confinement fusion (ICF) experiments, two-plasmon decay (TPD) is one of the crucial laser-plasma-instability (LPI) processes [1–4]. TPD is a three-wave parametric instability that occurs near the quarter-critical density surface in which an incident light wave decays into two electron plasma waves (EPWs) [5]. The TPD instability can absorb the energy of the incident laser, meanwhile the generated large-amplitude EPWs can transfer the energy to the electrons via Landau damping and accelerate electrons to high energies. In a shock ignition scheme, these energetic electrons by TPD could increase the pressure of the igniter shock and may benefit the launching of shock [6]. However in conventional direct-drive ICF, the hot-electrons can preheat the cold fuel and reduce the compressibility of the capsule [7,8]. Therefore, exploring the TPD instability is of great significance for ICF.

The theory of TPD instability including its growth rates, threshold, and saturation mechanism has been developed previously [9–13]. There are two types of unstable modes for TPD, including the absolute TPD modes localized close to the quarter-critical density surface and the convective TPD modes in the low-density regions [14]. And the hot electrons can be accelerated in stages from the low-density region to the high-density region [15]. Besides that, there are also several hot-electron acceleration mechanisms including Langmuir cavitation [16] and wave breaking [17] in the TPD process. In addition, the researchers are also concerned about the competition between TPD and other instabilities [18–20], and some schemes to mitigate TPD have been proposed, e.g., utilizing the broad-bandwidth laser [21,22] and improving the ablator materials [23,24].

Magnetic fields are widely present in laser plasmas; they are commonly accompanied by a self-generated magnetic field or an external magnetic field [25–31]. In recent years, more and more studies have utilized the external magnetic fields in ICF experiments to increase fuel temperature [28], affect implosion dynamics [29], and reduce hydrodynamic instabilities [30]. Additionally, many previous works have explored the effects of magnetic fields on the LPI process [32–40]. Particularly, the electrons trapped by EPWs achieve high energies through the surfatron acceleration when the EPW propagates perpendicular to the magnetic field [41,42]. The surfatron electron acceleration mechanism enhances the continual dissipation of EPWs, thus can be used to mitigate the stimulated Raman scattering (SRS) instability (the EPW is one of its daughter waves) [34–36]. There is also some research involving the TPD instability in magnetized plasmas, they obtained the growth rate and threshold of TPD in the magnetic field and indicated that the excitation of TPD is no longer restricted to the quarter-critical density surface in a ultrastrong (thousands of tesla) magnetic field [38–40]. However, there is still no clear understanding about the nonlinear evolution and the hot-electron generation of TPD in the magnetic fields.

It is well known that the two daughter waves of TPD are the forward EPW (FEPW) and the backward EPW (BEPW). The direction and magnitude of their phase velocity are

---

*liuzj@iapcm.ac.cn

different from each other and the phase velocity of FEPW is smaller than that of the BEPW. Naturally, the hot electrons generated by FEPW are not interfered by the BEPW in unmagnetized plasmas. In this Letter, we consider an external magnetic field perpendicular to the plane of the TPD wave vector and identify an anomalous staged hot-electron acceleration mechanism, i.e., the energetic electrons generated by the FEPW can be trapped and be accelerated again by the BEPW. Moreover, the surfatron acceleration mechanism of TPD in the magnetic field is also confirmed, the electrons trapped by the TPD daughter EPWs are accelerated perpendicularly across the wave front. It is interesting to note that the velocity of electrons accelerated by surfing from the FEPW is quite close to the BEPW phase velocity, these electrons can be easily accelerated again by the BEPW, which markedly enhances the efficiency of the staged acceleration. The coexistence of these two acceleration mechanisms leads to a significant increase of hot electrons generated by TPD under the action of a magnetic field. Meanwhile, the EPWs are dissipated and TPD is effectively suppressed. Since the EPW phase velocity of the convective TPD is lower than that of the absolute TPD, more electrons in the low-density region can be accelerated by surfing while the dissipation of EPWs is more stronger, making the convective TPD easier to suppress in the magnetic field. Additionally, it is shown that the magnetic field can increase the fraction of hot electrons and the laser transmission. The results help us to understand the impact of an external magnetic field on the evolution and the hot electron generation of TPD under the conditions related to ICF.

We carry out the two-dimensional (2D) simulations via particle-in-cell (PIC) code EPOCH [43] to study the effects of a transverse magnetic field with tens of tesla on the TPD instability and its hot-electron generation under the parameters of experiments at the OMEGA laser facility. Here, the simulation box is 40 μm in the longitudinal (x) direction and 10 μm in the transverse (y) direction with grids of 4000×1000. A collisionless, fully ionized CH plasma is initialized with 140 particles per cell for electrons and 20 for each ion species. Ions are mobile in the simulation, the masses of carbon and hydrogen ions are $12 \times 1836 m_e$ and $1836 m_e$ (m_e is the electron mass). The initial electron and both ion temperatures are $T_e = 2.0$ keV and $T_i = 0.5$ keV, respectively. The plasma has a linear density profile of $n_0(x) = 0.205 n_c (1 + x/150$ μm$)$ with the density variation range from $0.205 n_c$ to $0.259 n_c$, and the density scale length at the quarter-critical surface is $L_n = n_0(x)/[dn_0(x)/dx] |_{n_0=n_c/4} \approx 183$ μm. Here, n_c ($n_c \equiv 1.11 \times 10^{21}/\lambda_{0,\mu m}^2$ in cm^{-3}) denotes the critical density of the incident light with $\lambda_0 = 0.351$ μm. A p-polarized plane-wave laser with the intensity $I_0 = 8.0 \times 10^{14}$ W/cm^2 enters the box from the left boundary along the x direction, which has a ramp-up time of $18 T_0$ ($T_0 = \lambda_0/c \approx 1.17$ fs denotes the laser period, c is the light speed in vacuum) and is kept constant afterward. The total simulation time is $5200 T_0 \approx 6$ ps, during which the quasisteady states are reached. The absorbing boundary condition for the fields and the thermal boundary condition for the particles are applied in the longitudinal (x) direction, and the transverse (y) directions use the periodic boundary conditions for both fields and particles. In addition, the anomalous staged acceleration mechanism requires that the magnetic field must be perpendicular to the plane of TPD

wave vector and is set in the z direction here. The external magnetic field B_z ranging from 10 to 80 T is applied and remains as a constant of space-time. In this regime, $\omega_c \ll \omega_{pe}$ (ω_c and ω_{pe} are the electron cyclotron and plasma frequencies), so the influence of magnetic fields on the dispersion relations of electromagnetic waves and EPWs are negligible. Under the selected parameters above, the SRS instability is not observed in our simulations, since it tends to occur with a higher laser intensity and a longer density scale length [3,18,20].

Before discussing the anomalous staged acceleration mechanism, we consider a TPD daughter EPW of the form $E_L \sin(k_L R - \omega_L t)$ (k_L and ω_L are its wave number and frequency, respectively) propagates obliquely along the R direction in the x-y plane and is perpendicular to the uniform magnetic field B_z. $R_\perp$ is set to the direction along the wave front and is perpendicular to the magnetic field. It is convenient to use a wave frame to describe the electron moving in an electrostatic wave field, we transform the coordinates such that $r = R - v_{ph}t$ and $r_\perp = R_\perp$, where $v_{ph} = \omega_L/k_L$ is the phase velocity of EPW. Then, the equations of motion for trapped electrons in the wave frame are (ignore the high-frequency oscillation in the laser field)

$$\frac{d^2 r}{dt^2} = -\omega_c \left[\frac{dr_\perp}{dt} + \frac{E_L}{B_z} \sin(k_L r) \right], \quad (1)$$

$$\frac{d^2 r_\perp}{dt^2} = \omega_c \left(\frac{dr}{dt} + v_{ph} \right). \quad (2)$$

The derivative of Eq. (1) and the integration of Eq. (2) can be written as

$$\frac{d^3 r}{dt^3} = -\omega_T^2 \frac{dr}{dt} - \omega_c^2 v_{ph}, \quad (3)$$

$$\frac{dr_\perp}{dt} = \omega_c [(r - r_0) + v_{ph}t], \quad (4)$$

where $\omega_T^2 = \omega_c^2 + e k_L E_L \cos(k_L r)/m_e$ is the modified trapped electron bounce frequency. The electron executes bounce motion with the modified frequency ω_T while it is accelerated in the direction $r_\perp$, which is the surfatron electron acceleration mechanism. Equation (3) describes sinusoidal oscillations of dr/dt about an average velocity $v_r^{av} = -\omega_c^2/\omega_T^2 v_{ph}$. It means that the average velocity of the trapped electron is slower than the phase velocity of EPWs, and it increases to the rate of v_{ph} as $\cos(k_L r) \to 0$, at which time detrapping occurs and the condition $d^2 r/dt^2 \to 0$ should be met, one can get the escape velocity $v_{esc} = E_L/B_z$ in the direction $r_\perp$. However, if the electron starts at different locations in the potential well or begins with a large speed v_r, then it can escape with a value less than v_{esc} [34]. Furthermore, the amplitude and phase velocity of the EPWs are continually changing in the development of TPD instability and the detrapping is actually more complicated.

Observing the tracks of electrons in velocity space is a useful way to visually identify the process that how the electrons are accelerated. Two representative cases of one electron being accelerated in stages by the FEPW and BEPW of TPD successively in a magnetic field are shown in Figs. 1(a1) and 1(a2). In Fig. 1(a1), one unperturbed electron initially executes the cyclotron motion with a counterclockwise gyration
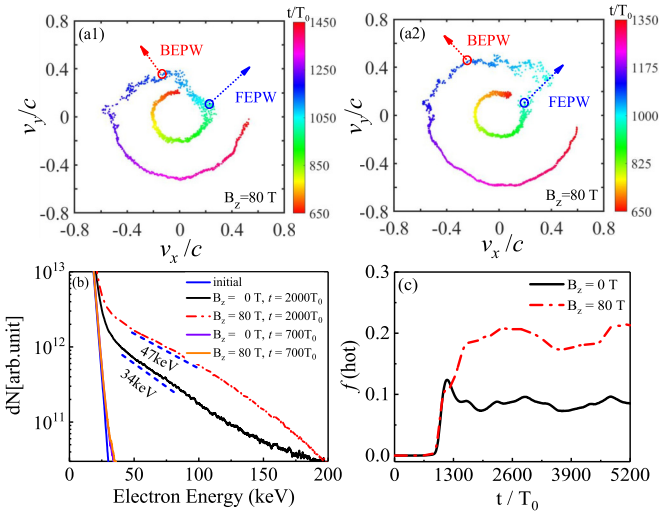
FIG. 1. (a1), (a2) The tracks of one electron display the staged acceleration process in $v_x - v_y$ space for $B_z = 80$ T. (a1) The staged acceleration is completed by the surfatron accelerations respectively from FEPW and BEPW of TPD. (a2) One electron is first accelerated along the direction of TPD FEPW and then is accelerated again in stages by the BEPW surfatron. (b) The electron energy spectra at different times for $B_z = 0$ T and $B_z = 80$ T. (c) The time evolutions of total hot-electron fraction for $B_z = 0$ T and $B_z = 80$ T.

in the magnetic field $B_z = 80$ T. Then, it is trapped when it moves near the TPD FEPW phase velocity $v_{ph-F} \approx 0.25c$ [$(v_x, v_y) = (0.23c, 0.10c)$] at about $t = 1050T_0$ and is accelerated by surfing from the FEPW in the direction along the wave front, thus also confirming the surfatron acceleration mechanism of TPD in the magnetic field. After about $50T_0$, the electron moves near the BEPW phase velocity $v_{ph-B} \approx 0.38c$ [$(v_x, v_y) = (-0.15c, 0.35c)$], it is trapped and has a surfatron acceleration again by the BEPW. Eventually, it executes the cyclotron motion with a higher velocity after escaping from the BEPW potential well. Interestingly, the velocity of the electron by the surfatron acceleration from the FEPW is quite close to the BEPW phase velocity, so they can be easily trapped in BEPW and accelerated again and the electron extracts a relatively high energy from EPWs in such the staged acceleration process. Furthermore, Fig. 1(a2) shows another special case of the staged acceleration mechanism in the magnetic field. It can be seen that when the cyclotron electron moves near the FEPW phase velocity $v_{ph-F} \approx 0.21c$ [$(v_x, v_y) = (0.19c, 0.09c)$] at about $t = 1000T_0$, the initial bounce frequency of the trapped electron satisfies $\omega_T \rightarrow \omega_c$, the electron acceleration in the direction $r_\perp$ is 0. Therefore, the trapped electron is first accelerated by the FEPW in the direction along the wave. After escaping, it continues to execute the cyclotron motion in a period of time until it moves near the BEPW phase velocity $v_{ph-B} \approx 0.50c$ [$(v_x, v_y) = (-0.23c, 0.44c)$] at about $t = 1120T_0$. Next, it can be clearly seen that the electron is accelerated again by surfing along the direction perpendicular to the BEPW. In the magnetic field, the coexistence of the staged acceleration mechanism and the surfatron acceleration mechanism enhances the efficiency of the hot electron generated by TPD and leads to a significant increase of energetic electrons.

Figure 1(b) plots the electron energy spectra at different times for $B_z = 0$ T and $B_z = 80$ T. Compared with the initial Maxwell distribution, there is almost no generation of hot electrons at $t = 700T_0$ in the linear stage of TPD, and the external magnetic field has almost no effect on the generation of the hot electrons in this stage. Note that a large number of hot electrons are generated at $t = 2000T_0$ during the nonlinear stage. Especially considering the external magnetic field, due to the coupling of the staged acceleration mechanism and the surfatron acceleration mechanism, the number of energetic electrons has a significant increase, and the effective temperature of hot electrons increases from 34 to 47 keV. In fact, it can be estimated from Figs. 1(a1) and 1(a2) that the velocities of eventual electron cyclotron motion are $0.52c$ and $0.58c$, respectively, after the staged acceleration, the corresponding energies are approximately 87 and 116 keV, which are in the region of increased energy in Fig. 1(b). The time evolutions of the total hot-electron fraction $f(\text{hot})$ with the kinetic energy higher than 50 keV in the simulation box are displayed in Fig. 1(c) for $B_z = 0$ T and $B_z = 80$ T. It can be seen that when considering the external magnetic field, the fraction of hot electrons increases significantly compared with without magnetic field. By averaging the fraction in the nonlinear stage ($t = 800T_0–5200T_0$) of TPD, it can be estimated that the hot-electron fraction increases from 8% to 18% under the action of a magnetic field, it has more than doubled. However, it cannot be concluded that the magnetic field can enhance the target preheating and is detrimental for direct drive. For the TPD instability in unmagnetized plasmas, it is general to count the hot electrons on the right boundary to care about the target preheating. After considering the magnetic field, it should be noted that the trapped hot electrons can be accelerated in the direction perpendicular to the EPWs due to the surfatron acceleration mechanism and will execute the cyclotron motion in the magnetic field after escaping from the EPW potential well. Finally, the motion of hot electrons in the magnetic field no longer has a clear direction and will be filled with all directions in the v_x-v_y phase space. We have reason to believe that the larger simulation box will effectively limit the hot electrons moving towards the right boundary due to the captivity effect of the magnetic field, resulting in a decrease of target preheating. Just as the research by Yao *et al.* indicates, the transverse magnetic field can make the hot-electron confinement and reduce the target preheating [37].

Moreover, when the large-amplitude EPWs propagate perpendicular to the magnetic field, the electrons trapped in EPWs are accelerated by surfing meanwhile continuously extracting energy from EPWs. The surfatron electron acceleration mechanism of TPD enhances the dissipation of EPWs, forming the effect of wave damping, which can result in the suppression of TPD instability. Figures 2(a1) and 2(a2) describe the spatial-temporal evolutions of the transverse averaged longitudinal electric-field energy $\langle E_x^2 \rangle = \int E_x^2 dy / \int dy$ in the system for $B_z = 0$ T and $B_z = 80$ T, respectively. It can be seen from Fig. 2(a1) that, in the linear stage of TPD with the OMEGA parameters, the absolute TPD near the quarter-critical density surface is in a dominant regime. As TPD saturates at $t = 800T_0$, the ion density fluctuations driven by the plasma waves will drive the development of
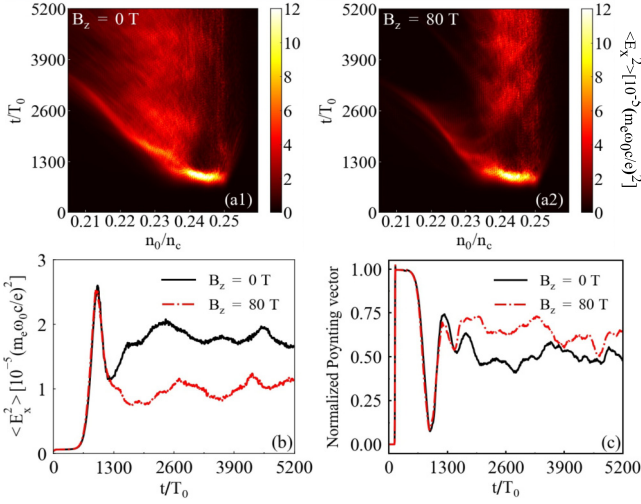
FIG. 2. (a1), (a2) The spatial-temporal evolutions of the transverse averaged longitudinal electric-field energy for different magnetic fields. (a1) $B_z = 0$ T, (a2) $B_z = 80$ T. (b) The time evolution of the averaged longitudinal electric-field energy (integrated in the entire simulation box). (c) The time evolutions of the averaged normalized Poynting vector at the right boundary.
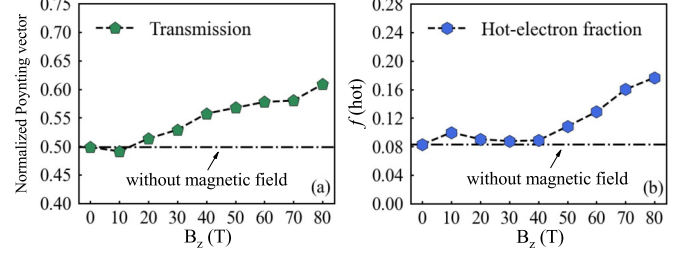

FIG. 3. (a), (b) The normalized transmitted laser Poynting vector and the total hot-electron fractions averaged over $t = 800T_0$ to $t = 5200T_0$ as a function of magnetic field.

convective TPD in the low-density region (roughly from $0.205n_c$ to $0.24n_c$) [15]. It is significantly excited at about $t \approx 1400T_0$, corresponding to the second-weaker burst in Fig. 2(a1), and then the longitudinal electric-field energy reaches a steady state. After considering the external magnetic field [see Fig. 2(a2)], TPD is significantly suppressed, especially the convective TPD. Because the convective TPD in the low-density region has a smaller phase velocity, the kinetic effect is stronger and the wave-particle interaction is more obvious, the number of trapped electrons is more than the absolute TPD. Naturally, more electrons can be accelerated by surfing in the magnetic field and extract a relatively high energy from EPWs, so the dissipation of convective TPD is stronger than the absolute TPD, which makes the convective TPD more sensitive to the magnetic field than the absolute TPD. Finally, the convective TPD is continuously suppressed and a quasisteady state is also reached in the magnetic field. Additionally, more laser energy can be transmitted to the region near the quarter-critical density surface as the pump dissipation weakens in the low-density region, resulting in a slight enhancement of the absolute TPD compared with the unmagnetized plasma. Figure 2(b) shows the time evolutions of the averaged longitudinal electric-field energy (integrated in the entire simulation box) corresponding to Figs. 2(a1) and 2(a2). It can be clearly seen that the magnetic field has almost no effect on the evolution of TPD in the linear stage, because there are few hot-electron generation [see Figs. 1(b) and 1(c)], in which stage the surfatron acceleration efficiency is extremely low. In the nonlinear stage, as the number of hot electrons generated by TPD increases, the efficiency of staged acceleration and surfatron acceleration enhances and the EPWs are dissipated, leading to a significant suppression of TPD. In addition, we are also concerned about the laser transmission, Fig. 2(c) show that the time evolutions of the

averaged normalized Poynting vector in the x direction at the right boundary for $B_z = 0$ T and $B_z = 80$ T. Combined with Fig. 2(b), it can be found that the laser is absorbed with the increase of TPD instability, which makes the laser transmission decrease markedly. When TPD enters the saturation stage, the laser transmission rises and finally reaches the quasisteady state. From Fig. 2(c), it can be estimated that the average transmission of laser in the nonlinear stage without the magnetic field is around 50%. Due to the suppression of TPD instability by the external magnetic field, the averaged laser transmission is raised to around 62%.

In Fig. 3, we present the normalized transmitted laser Poynting vector in the x direction at the right boundary and the total hot-electron fractions averaged over $t = 800T_0$–$5200T_0$ as a function of magnetic field. It can be seen that in overall situation, whether the laser transmission or the fraction of hot electrons, both of them increase with the enhancement of magnetic field, which is due to the fact that the efficiency of surfatron acceleration increases with the magnetic field [34,35]. Comparing Figs. 3(a) and 3(b), it is found that the laser transmissivity has an enhancement in the weak magnetic field ($B_z \leqslant 40$ T), however the fraction of hot electrons with energies $E > 50$ keV still has no significant increase. It is indicated that some electrons have already been accelerated through the surfatron mechanism, resulting in a suppression of the TPD instability and an enhancement of the laser transmission. However, the velocity of most surfatron electrons from FEPW is not being accelerated to $0.41c$ (corresponding to the energy with 50 keV) due to the lower efficiency of surfatron acceleration in a weak magnetic field, it is difficult to reach near the phase velocity of BEPW, resulting the difficulty of the staged acceleration process. When the magnetic field becomes stronger ($B_z > 40$ T), there are more electron velocities close to the BEPW phase velocity as the efficiency of the surfatron acceleration enhances, making the further staged acceleration play an important role. The coupling effect of these two acceleration mechanisms results in a rapid increase of hot-electron fraction. In addition, the Larmor radius of electrons becomes larger as the magnetic field decreases. Therefore, the staged acceleration process shown in Fig. 1(a2) is almost nonexistent in systems with the weaker magnetic field, moreover the electrons are also likely to leave the boundary in this situation. On the contrary, as the Larmor radius gradually becomes smaller with the magnetic field, the efficiency of staged acceleration increases gradually, it also lead to an

increase in the fraction of hot electrons. Note that according to the maximum magnetic field $B_z = 80$ T in this Letter, the Larmor radius for the hot electrons of 50 keV is around 10 μm. In our simulation box, most of the hot electrons easily leave the boundary, which can truly characterize the physical process of the increase of hot electrons caused by the staged acceleration and surfatron acceleration. These results indicate that in the external transverse magnetic field of tens of tesla which can be achieved in ICF experiments, the anomalous staged acceleration mechanism and the surfatron acceleration existed in the TPD instability are important and cannot be ignored.

In summary, we present and identify a new hot-electron acceleration mechanism that the hot electrons generated by the TPD instability can be first accelerated by the FEPW and then by the BEPW again in a transverse magnetic field. Moreover, the surfatron acceleration mechanism of TPD in the magnetic field is also confirmed. The velocity of electrons accelerated by surfing from the FEPW is quite close to the BEPW phase

velocity, so these electrons can be easily accelerated again by the BEPW, which also dramatically enhances the efficiency of the staged acceleration. The coexistence of these two acceleration mechanisms leads to a significant increase of hot electrons generated by TPD in the magnetic field. Meanwhile the EPWs are dissipated and TPD instability is effectively suppressed. Particularly, the convective TPD is more sensitive to the magnetic field and easier to be suppressed compared with the absolute TPD. In addition, the simulation results also indicate that whether the hot-electron fraction or the laser transmission, both them increase with the enhancement of magnetic field. The results can provide a potential reference value for the evolution and the hot-electrons generation of TPD under the conditions related to ICF in magnetized plasmas.

[1] D. H. Froula, B. Yaakobi, S. X. Hu, P. Y. Chang, R. S. Craxton, D. H. Edgell, R. Follett, D. T. Michel, J. F. Myatt, W. Seka *et al.*, Phys. Rev. Lett. **108**, 165003 (2012).

[2] W. Seka, J. F. Myatt, R. W. Short, D. H. Froula, J. Katz, V. N. Goncharov, and I. V. Igumenshchev, Phys. Rev. Lett. **112**, 145001 (2014).

[3] M. J. Rosenberg, A. A. Solodov, J. F. Myatt, W. Seka, P. Michel, M. Hohenberger, R. W. Short, R. Epstein, S. P. Regan, E. M. Campbell *et al.*, Phys. Rev. Lett. **120**, 055001 (2018).

[4] R. H. H. Scott, K. Glize, L. Antonelli, M. Khan, W. Theobald, M. Wei, R. Betti, C. Stoeckl, A. G. Seaton, T. D. Arber *et al.*, Phys. Rev. Lett. **127**, 065001 (2021).

[5] W. L. Kruer, *The Physics of Laser Plasma Interactions* (Addison-Wesley, Redwood City, 1988).

[6] W. L. Shang, R. Betti, S. X. Hu, K. Woo, L. Hao, C. Ren, A. R. Christopherson, A. Bose, and W. Theobald, Phys. Rev. Lett. **119**, 195001 (2017).

[7] V. A. Smalyuk, D. Shvarts, R. Betti, J. A. Delettrez, D. H. Edgell, V. Yu. Glebov, V. N. Goncharov, R. L. McCrory, D. D. Meyerhofer, P. B. Radha *et al.*, Phys. Rev. Lett. **100**, 185005 (2008).

[8] J. A. Delettrez, T. J. B. Collins, and C. Ye, Phys. Plasmas **26**, 062705 (2019).

[9] M. N. Rosenbluth, Phys. Rev. Lett. **29**, 565 (1972).

[10] R. Yan, A. V. Maximov, and C. Ren, Phys. Plasmas **17**, 052701 (2010).

[11] A. Simon, R. W. Short, E. A. Williams, and T. Dewandre, Phys. Fluids **26**, 3107 (1983).

[12] B. B. Afeyan and E. A. Williams, Phys. Plasmas **4**, 3803 (1997).

[13] A. B. Langdon, B. F. Lasinski, and W. L. Kruer, Phys. Rev. Lett. **43**, 133 (1979).

[14] R. Yan, A. V. Maximov, C. Ren, and F. S. Tsung, Phys. Rev. Lett. **103**, 175002 (2009).

[15] R. Yan, C. Ren, J. Li, A. V. Maximov, W. B. Mori, Z. M. Sheng, and F. S. Tsung, Phys. Rev. Lett. **108**, 175002 (2012).

[16] H. X. Vu, D. F. DuBois, D. A. Russell, and J. F. Myatt, Phys. Plasmas **19**, 102708 (2012).

[17] T. P. Coffey, Phys. Fluids **14**, 1402 (1971).

[18] C. Z. Xiao, Z. J. Liu, C. Y. Zheng, and X. T. He, Phys. Plasmas **23**, 022704 (2016).

[19] H. Wen, A. V. Maximov, R. Yan, J. Li, C. Ren, and F. S. Tsung, Phys. Rev. E **100**, 041201(R) (2019).

[20] C. Z. Xiao, H. B. Zhuo, Y. Yin, Z. J. Liu, C. Y. Zheng, and X. T. He, Nucl. Fusion **60**, 016022 (2020).

[21] R. K. Follett, J. G. Shaw, J. F. Myatt, J. P. Palastro, R. W. Short, and D. H. Froula, Phys. Rev. Lett. **120**, 135005 (2018).

[22] R. K. Follett, J. G. Shaw, J. F. Myatt, C. Dorrer, D. H. Froula, and J. P. Palastro, Phys. Plasmas **26**, 062111 (2019).

[23] V. A. Smalyuk, R. Betti, J. A. Delettrez, D. D. Meyerhofer, P. B. Radha, S. P. Regan, T. C. Sangster, J. Sanz, W. Seka *et al.*, Phys. Rev. Lett. **104**, 165002 (2010).

[24] R. K. Follett, J. A. Delettrez, D. H. Edgell, V. N. Goncharov, R. J. Henchen, J. Katz, D. T. Michel, J. F. Myatt, J. Shaw, A. A. Solodov *et al.*, Phys. Rev. Lett. **116**, 155002 (2016).

[25] I. V. Igumenshchev, A. B. Zylstra, C. K. Li, P. M. Nilson, V. N. Goncharov, and R. D. Petrasso, Phys. Plasmas **21**, 062707 (2014).

[26] V. V. Ivanov, A. V. Maximov, R. Betti, L. S. Leal, J. D. Moody, K. J. Swanson, and N. A. Huerta, Matter Radiat. Extrem. **6**, 046901 (2021).

[27] Y. Shi, A. Arefiev, J. X. Hao, and J. Zheng, Phys. Rev. Lett. **130**, 155101 (2023).

[28] D. S. Montgomery, B. J. Albright, D. H. Barnak, P. Y. Chang, J. R. Davies, G. Fiksel, D. H. Froula, J. L. Kline, M. J. MacDonald, A. B. Sefkow *et al.*, Phys. Plasmas **22**, 010703 (2015).

[29] P. Y. Chang, G. Fiksel, M. Hohenberger, J. P. Knauer, R. Betti, F. J. Marshall, D. D. Meyerhofer, F. H. Séguin, and R. D. Petrasso, Phys. Rev. Lett. **107**, 035006 (2011).

[30] L. J. Perkins, D. D.-M. Ho, B. G. Logan, G. B. Zimmerman, M. A. Rhodes, D. J. Strozzi, D. T. Blackfield, and S. A. Hawkins, Phys. Plasmas **24**, 062708 (2017).

[31] W. Yao, A. Fazzini, S. N. Chen, K. Burdonov, P. Antici, J. Béard, S. Bolaños, A. Ciardi, R. Diab, E. D. Filippov *et al.*, Matter Radiat. Extrem. **7**, 014402 (2022).

[32] Z. J. Liu, B. Li, J. Xiang, L. H. Cao, C. Y. Zheng, and L. Hao, Plasma Phys. Control. Fusion **60**, 045008 (2018).

[33] M. R. Edwards, Y. Shi, J. M. Mikhailova, and N. J. Fisch, Phys. Rev. Lett. **123**, 025001 (2019).

[34] B. J. Winjum, F. S. Tsung, and W. B. Mori, Phys. Rev. E **98**, 043208 (2018).

[35] Y. Z. Zhou, C. Y. Zheng, Z. J. Liu, and L. H. Cao, Plasma Phys. Control. Fusion **63**, 055015 (2021).

[36] M. Bailly-Grandvaux, B. J. Winjum, M. J.-E. Manuel, S. Bolaños, C. A. Walsh, J. Saret, A. Bogale, J. Strehlow, R. Lee, F. Tsung *et al.*, J. Plasma Phys. **89**, 175890201 (2023).

[37] W. Yao, A. Higginson, J.-R Marquès, P. Antici, J. Béard, K. Burdonov, M. Borghesi, A. Castan, A. Ciardi, B. Coleman *et al.*, Phys. Rev. Lett. **130**, 265101 (2023).

[38] H. C. Barr, T. J. M. Boyd, L. R. T. Gardner, and R. Rankin, Phys. Fluids **27**, 2730 (1984).

[39] N. M. Laham, A. M. Al-khateeb, A. S. Al Nasser, and I. M. Odeh, Phys. Plasmas **7**, 3993 (2000).

[40] A. Panwar and A. K. Sharma, Phys. Scr. **75**, 439 (2007).

[41] J. M. Dawson, V. K. Decyk, Robert W. Huff, I. Jechart, T. Katsouleas, J. N. Leboeuf, B. Lembege, R. M. Martinez, Y. Ohsawa, and S. T. Ratliff, Phys. Rev. Lett. **50**, 1455 (1983).

[42] T. Katsouleas and J. M. Dawson, Phys. Rev. Lett. **51**, 392 (1983).

[43] T. D. Arber, K. Bennett, C. S. Brady, A. Lawrence-Douglas, M. G. Ramsay, N. J. Sircombe, P. Gillies, R. G. Evans, H. Schmitz, A. R. Bell *et al.*, Plasma Phys. Control. Fusion **57**, 113001 (2015).